Journal of
Nanoscience and Nanotechnology
Vol. 13, 1769–1772, 2013

Nanocomposites of Polystyrene/Polystyrene-Grafted Graphene Oxides Synthesized by *In-Situ* Bulk Polymerization

Jaehoon Lee, Young Soo Yun, Do Hyeong Kim, Hyun Ho Park, and Hyoung-Joon Jin*

Department of Polymer Science and Engineering, Inha University, Incheon 402-751, Republic of Korea

In this study, polystyrene-grafted graphene oxide (GO-*g*-PS) nanocomposites with different PS chain lengths were prepared by *in-situ* polymerization, and their reinforcing effect on the PS matrix was investigated. The glass transition (T_g) and the thermal degradation (T_d) temperatures of the PS/GO-*g*-PS nanocomposites were increased up to 2.8 °C and 23.9 °C, respectively. The addition of only 0.1 wt% of the GO-*g*-PS to the PS/GO-*g*-PS nanocomposites increased the tensile strength and Young's modulus by around 20.5% and 71.4%, respectively. These results showed that the thermal and mechanical properties of the PS/GO-*g*-PS nanocomposites gradually improved with increasing length of the PS chain grafted onto the GO surface. These differences in reinforcing effects were attributed to differences in interfacial interaction between the graphene and PS matrix.

Keywords: Graphene, Polystyrene, Polymer-Grafted Graphene Oxide, Interfacial Interaction.

RESEARCH ARTICLE

1. INTRODUCTION

Graphene, characterized by an atomically thin, two-dimensional sheet of a hexagonal lattice-like honey comb, has attracted significant attention in recent years due to its unique and remarkable properties.[1] Graphene is considered useful in various technological areas, such as electronics, sensors, solar cells, memory devices, hydrogen storage, and polymer nanocomposites, because of its well-defined thermal conductivity, electrical conductivity, high surface area, and excellent mechanical strength.[2, 3] However, the application of these beneficial properties to polymer nanocomposites requires that the graphene is homogeneously dispersed onto the polymeric matrices. Therefore, preventing aggregation of the graphene layers in polymer matrices is crucial in the field of nanotechnology because most of their unique properties are only associated with thicknesses of a few layers or even individual sheets.[4, 5]

The most common approach for the exfoliation and dispersion of graphene is the oxidation of graphite to form graphite oxide.[6–8] Graphite oxide is hydrophilic and is easily exfoliated in water and other solvents as single sheets, termed graphene oxide (GO). The presence of the epoxide, carboxyl and hydroxyl groups on the basal plane and edge of GO reduces the interlayer forces and renders them soluble in water and polar solvents such as dimethylformamide (DMF).[9] In contrast, organic molecules such as phenyl isocyanate[10] and porphyrin[11] have also been attached to graphene surfaces to improve dispersion in non-polar solvents such as toluene. These approaches have been employed to improve the dispersion of graphene nanosheets in polymer nanocomposites.[3, 12] However, there are some difficulties in improving the graphene-polymer interfacial adhesion because of the small size of the molecule.[4] To overcome this problem, poly(vinyl chloride) (PVC) has been used to covalently functionalize graphene by esterification of isocyanate-modified GO with appropriately modified PVC.[13] Fang et al. showed that the initiator molecules were covalently bonded to the graphene surface via diazonium addition and that the succeeding atom transfer radical polymerization linked polystyrene (PS) chains to the graphene nanosheets.[14] Consequently, the production of graphene nanosheets with appropriate surface chemistry for the fabrication of graphene-based polymer nanocomposites is very desirable.

In this study, GO-*g*-PS nanocomposites with different PS chain lengths were prepared by *in-situ* polymerization, and their reinforcing effects on the PS matrix were investigated. The thermal and mechanical properties of the PS/GO-*g*-PS nanocomposites were gradually improved with increasing chain length of the grafted PS.

*Author to whom correspondence should be addressed.

These results indicate that interfacial interaction between the graphene filler and the PS matrix was increased with increasing chain length of the grafted PS.

2. EXPERIMENTAL DETAILS

2.1. Preparation of Graphene Oxide Alkylated with 4-Vinylbenzyl Chloride (VB-GO)

The graphite powder was oxidized and exfoliated into GO using a modified Hummers method,[6–8] in which 100 mg of the GO powder was exfoliated by ultrasonication in 180 mL of deionized water containing 72 mg of NaOH. Subsequently, 100 mg of a phase transfer agent, tetra-*n*-octylammonium bromide (TOAB, Fluka), and 5.0 mL of 4-vinylbenzyl chloride (Aldrich, 98%) were added to the black homogeneous sodium salt mixture. After stirring for 12 h at 90 °C, a black precipitate was obtained. The precipitate was filtered with excess chloroform, washed several times with a 15% NaCl aqueous solution and dried under vacuum.

2.2. Synthesis of Polystyrene-Grafted Graphene Oxide (GO-*g*-PS)

In-situ radical polymerization experiments were carried out in a 250 ml bottom flask at a vinylbenzyl-graphene oxide (VB-GO) content of 0.01 wt% with reference to styrene. The initiator, AIBN, was charged into the reactor just before the start of the polymerization at a fixed concentration of 0.1 mol% with reference to styrene. The system was maintained at 70 °C for 24 h, 36 h, and 48 h, including an agitation period maintained at 100 rpm for the first 6 h. The GO-*g*-PS nanocomposites with various polymerization times were dissolved in chloroform. Ultrasonication (600 W, 28 kHz, 2 h) of these GO-*g*-PS solutions in a water bath produced dark suspensions, some of which were filtrated with a 450 nm polytetrafluoroethylene membrane to collect the GO-*g*-PS filtrate. The filtrate containing PS from the filtration of the GO-*g*-PS was precipitated in excessive ethanol and dried at 60 °C under vacuum for gel permeation chromatography (GPC) measurements. After filtration, the product was purified twice by dissolution-precipitation with methanol and dried at 60 °C for 24 h under vacuum. The gray solid obtained by filtration was washed with DMF (100 mL) three times and dried at 60 °C under vacuum.

2.3. Characterization

The structures of GO, VB-GO and GO-*g*-PS were measured using Fourier transform infrared spectroscopy (FT-IR, vertex 80 v, Bruker Optics, Germany). Differential scanning calorimetry (DSC, Perkin Elmer Jade, USA) was carried out in dry nitrogen gas at a flow rate of 10 mL/min. The DSC was calibrated using indium as the standard, and the sample weight was 7.0 ± 0.1 mg. The thermal history of the PS/GO-*g*-PS nanocomposite was removed by scanning them from at temperatures ranging from 25 °C to 260 °C at a heating rate of 10 °C/min, followed by cooling to 25 °C at a scan rate of 10 °C/min. The quantity of PS chains grafted onto GO and the thermal degradation behavior of the nanocomposites were calculated by thermogravimetric analysis (TGA, Q50, TA instruments, UK) at temperatures ranging from 25 °C to 800 °C at a heating rate of 10 °C/min in a nitrogen atmosphere. The tensile properties were tested using an Instron 4665 ultimate tensile testing machine (UTM) at a temperature of 20 °C and a humidity of 30%. The dumb-bell specimens were made according to the ASTM D 638 standard for tensile testing. The cross-head speed was set to 50 mm/min for both dumb-bell samples. The mean value of each product was determined as the average value of five test specimens.

3. RESULTS AND DISCUSSION

The GO with 4-vinylbenzyl chloride was processed so that the vinyl group was covalently linked to the GO surface. Subsequently, *in-situ* radical polymerization allowed PS chains to grow from the VB-GO surface, as shown in Figure 1. The figure also depicts how the length of the polymer chain was controlled by applying different radical polymerization times. Table I shows the reaction conditions and summarizes the experimental results. With increasing polymerization time, the number-average molecular weight (M_n) of the grafted PS was increased from 70,905 to 121,997.

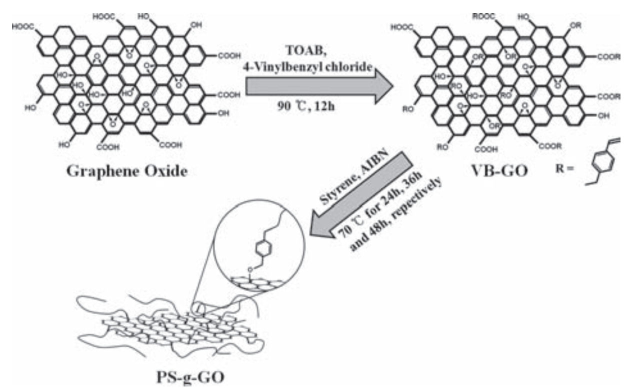

Fig. 1. Synthesis route of the GO-*g*-PS.

Table I. Reaction conditions and experimental results of the different GO-*g*-PS nanocomposites.

Sample name	Polymerization time (h)	M_n	WL (wt%)
GO-*g*-PS (24 h)	24	70,905	46.9
GO-*g*-PS (36 h)	36	96,783	64.1
GO-*g*-PS (48 h)	48	121,997	89.8

Note: WL: weight loss at 700 °C.

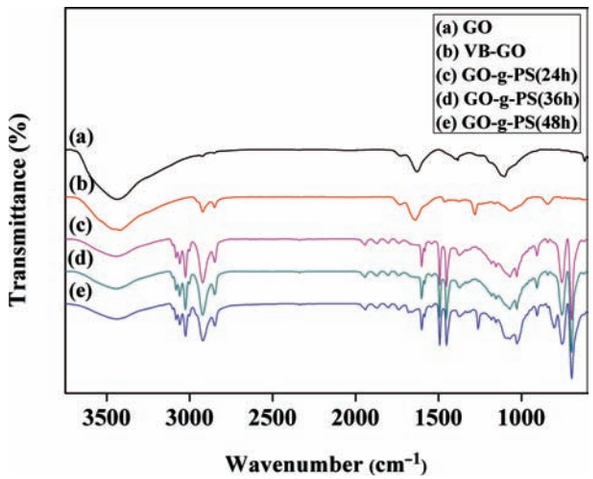

Fig. 2. FT-IR spectra of GO (a), VB-GO (b), GO-*g*-PS (24 h) (c), GO-*g*-PS (36 h) (d), and GO-*g*-PS (48 h) (e).

FT-IR spectroscopy was used to elucidate the covalent attachment between the GO and the functional group. Figure 2 shows the spectra of GO, VB-GO, and GO-*g*-PS. For the GO, the peaks at 3441 cm^{-1} were attributed to the hydroxyl stretch-ing vibrations of the C–OH groups, while a weak band at 1732.4 cm^{-1} and a strong band at 1628.8 cm^{-1} were both attributed to the C═O stretching vibrations of the –COOH groups. A band at 1387 cm^{-1} was attributed to the O–H deformations of the C–OH groups, and a strong band at 1100 cm^{-1} to C–O stretching vibrations.[15] However, for the VB-GO, the new band appearing at 840 cm^{-1} was assigned to para-substituted aromatic rings. These results indicate that the vinylbenzyl group was successfully attached on the GO surface. These vinylbenzyl groups render VB-GO hydrophobic, which allows the VB-GO to disperse in styrene monomer during *in-situ* polymerization.[16] In the spectra of the GO-*g*-PS nanocomposites, the absorption peaks at 3026, 2921, 1603, 1493, 1450, 1025, 752 and 693 cm^{-1} were evidence of the PS chains grafted onto the GO surface.

We can calculate the quantity of grafted PS on GO by TGA and the results are shown in Table I. In the case of the GO-*g*-PS, the weight loss of the samples reached equilibrium at a temperature of 600 °C. The weight loss was attributed to the presence of grafted PS on the GO surface. The quantity of grafted PS on the GO surface was 46.9 wt% for the GO-*g*-PS (24 h), 64.1 wt% for the GO-*g*-PS (36 h) and 89.8 wt% for the GO-*g*-PS (48 h). The results showed that an increase of the radical polymerization time facilitated control of the grafted PS on the GO surface. For the GO-*g*-PS nanocomposite samples, the thermal stability was gradually improved with increasing M_n of the grafted PS. This improvement indicates that the grafted PS layer inhibited decomposition of residual groups on the GO surface, due to the larger coverage ratios and thicker polymer layers.

Table II. Thermal and mechanical properties of pristine PS and PS nanocomposites containing 0.1 wt% of VB-GO and 0.1 wt% of GO-*g*-PS (T_d: 20 wt% loss).

Sample name	Strain at max (%)	Tensile strength (MPa)	Young's modulus (GPa)	T_g (°C)	T_d (°C)
PS	2.4 ± 0.2	37.6 ± 1.6	0.7	104.7	409.2
PS/VB-GO	2.1 ± 0.3	35.8 ± 2.1	0.9 ± 0.1	105.3	415.7
PS/GO-*g*-PS (24 h)	2.3 ± 0.4	42.1 ± 1.2	1.1 ± 0.1	105.8	420.7
PS/GO-*g*-PS (36 h)	2.4 ± 0.4	43.6 ± 1.6	1.1 ± 0.1	106.4	427.9
PS/GO-*g*-PS (48 h)	2.4 ± 0.4	45.3 ± 1.9	1.2 ± 0.1	107.5	433.1

The thermal and mechanical properties of the nanocomposites containing 0.1 wt% VB-GO and 0.1 wt% GO-*g*-PS are shown in Table II. Young's modulus of the PS/VB-GO was markedly increased. However, the tensile strength and strain at maximum were decreased compared to those of pristine PS. For the PS/GO-*g*-PS nanocomposites, however, the tensile strength and Young's modulus were remarkably enhanced. For the nanocomposite containing 0.1 wt% GO-*g*-PS (48 h), the tensile strength and Young's modulus were increased to 45.3 ± 1.9 MPa and 1.2 GPa, corresponding to increases of 20.5% and 66.9%, respectively (relative to the pristine PS). This suggests that the GO-*g*-PS was performed better in regard to load transfer than the VB-GO.[17] The glass transition temperature (T_g) of the PS/GO-*g*-PS nanocomposite was clearly shifted to a relatively high temperature region compared to that of pristine PS. The T_g of the PS/GO-*g*-PS (48 h) nanocomposite was increased by over 2.8 °C, which was attributed to the strong confinement effect of the chains to the particles that slowed the dynamics due to increased interfacial interactions (interpenetration) with the host chains[18]. Consequently, the PS/GO-*g*-PS (48 h) nanocomposite exhibited the largest T_g increase among the nanocomposites. In addition, the thermal degradation temperatures (T_d) of the PS/VB-GO and the PS/GO-*g*-PS nanocomposites increased. The mass loss of the pristine PS curve showed a 20 wt% loss at approximately 409 °C. However, T_d of the PS nanocomposites containing 0.1 wt% VB-GO and 0.1 wt% GO-*g*-PS (48 h) was increased by more than 6.5 °C and 23.9 °C compared to the pristine PS, respectively. These results were caused by the ability of the VB-GO and the GO-*g*-PS to restrict the mobilization of PS macromolecules, which resulted in homogeneous heating. This revealed a strong interfacial interaction between the GO-*g*-PS and the PS matrix.

4. CONCLUSION

The reinforcing effects of the PS/GO-*g*-PS nanocomposites with different PS chain lengths ($M_n = 70,905, 96,783$ and $121,997$) on the PS matrix were investigated. The thermal and mechanical properties of the PS nanocomposites with 0.1 wt% GO-*g*-PS were enhanced with increasing

chain length of the grafted PS. The tensile strength and Young's modulus of the PS nanocomposite containing only 0.1 wt% GO-*g*-PS (48 h) ($M_n = 121,997$) were increased by around 20.5% and 71.4%, respectively. In addition, T_g and T_d of the PS nanocomposite containing 0.1 wt% GO-*g*-PS (48 h) were increased by more than 2.8 °C and 23.9 °C compared to pristine PS, respectively. However, the thermal and mechanical properties of the PS/GO-*g*-PS (24 h) ($M_n = 70,905$) and the PS/GO-*g*-PS (36 h) ($M_n =$ 96,783) nanocomposites were not enhanced to the same extent as they were for the PS/GO-*g*-PS (48 h) nanocomposite. These results indicated that interfacial interaction between the graphene filler and PS matrix was increased with increasing chain length of the grafted PS.

Acknowledgment: This research was supported by Basic Science Research Program through the National Research Foundation of Korea(NRF) funded by the Ministry of Education, Science and Technology (R11-2005-065).

References and Notes

1. J. I. Paredes, S. Villar-Rodil, A. Martínez-Alonso, and J. M. D. Tascón, *Langmuir* 24, 10560 **(2008)**.
2. N. R. Wilson, P. A. Pandey, R. Beanland, R. J. Young, I. A. Kinloch, L. Gong, Z. Liu, K. Suenaga, J. P. Rourke, S. J. York, and J. Sloan, *ACS Nano* 3, 2547 **(2009)**.
3. J. R. Potts, S. H. Lee, T. M. Alam, J. An, M. D. Stoller, R. D. Piner, and R. S. Ruoff, *Carbon* 49, 2615 **(2011)**.
4. M. Fang, K. Wang, H. Lu, Y. Yanga, and S. Nuttb, *J. Mater. Chem.* 20, 1982 **(2010)**.
5. Y. K. Kim, M. H. Kim, and D. H. Min, *Chem. Commun.* 47, 3195 **(2011)**.
6. S. Stankovich, D. A. Dikin, R. D. Piner, K. A. Kohlhaas, A. Kleinhammes, Y. Jia, Y. Wu, S. T. Nguyen, and R. S. Ruoff, *Carbon* 49, 1588 **(2007)**.
7. S. Park, J. An, I. Jung, R. D. Piner, S. J. An, X. Li, A. Velamakanni, and R. S. Ruoff, *Nano Lett.* 9, 1593 **(2009)**.
8. I. Jung, D. Dikin, S. Park, W. Cai, S. L. Mielke, and R. S. Ruoff, *J. Phys. Chem. C* 112, 20264 **(2008)**.
9. Y. Si and E. T. Samulski, *Nano Lett.* 8, 1679 **(2008)**.
10. S. Stankovich, R. D. Piner, S. T. Nguyen, and R. S. Ruoff, *Carbon* 44, 3342 **(2006)**.
11. B. Y. Xu, Z. Liu, X. Zhang, Y. Wang, J. Tian, Y. Huang, Y. Ma, X. Zhang, and Y. Chen, *Adv. Mater.* 21, 1275 **(2009)**.
12. H. He and C. Gao, *Chem. Mater.* 22, 5054 **(2010)**.
13. H. J. Salavagione and G. Martínez, *Macromolecules* 44, 2685 **(2011)**.
14. M. Fang, K. Wang, H. Lu, Y. Yanga, and S. Nutt, *J. Mater. Chem.* 19, 7089 **(2009)**.
15. G. Wang, B. Wang, J. Park, J. Yang, X. Shen, and J. Yao, *Carbon* 47, 68 **(2009)**.
16. Y. S. Yun, Y. H. Bae, D. H. Kim, J. Y. Lee, I. J. Chin, and H. J. Jin, *Carbon* 49, 3553 **(2011)**.
17. S. Wang, R. Liang, B. Wang, and C. Zhang, *Chem. Phys. Lett.* 457, 371 **(2008)**.
18. H. Oh and P. F. Green, *Nat. Mater.* 8, 139 **(2009)**.

Received: 9 November 2011. Accepted: 22 February 2012.